ACCEPTED

Electromagnetic Classification

Ergun Simsek
University of Maryland Baltimore County, Baltimore, MD, USA (simsek@umbc.edu)

***Abstract*—Rather than reconstructing the properties or parameters of a medium as it is done in electromagnetic inversion, this work aims to classify objects with neural networks that are trained with scattered field data and labels (classes). The study demonstrates the feasibility of achieving an 86% accuracy, showcasing potential applications in robotics and environmental perception.**

I. Introduction

Electromagnetic inversion [1]–[3] refers to the process of reconstructing the properties or parameters of a medium (such as the distribution of electrical permittivity or conductivity) from the measurements of electromagnetic fields scattered or transmitted through the medium as depicted in Fig. 1(a). The primary goal of electromagnetic inversion is to infer the internal structure or composition of an object or a material by analyzing how it interacts with incident electromagnetic waves, see Fig. 1(b) as an example. This is particularly important in fields like geophysics, medical imaging, and non-destructive testing. Traditional methods face challenges such as nonlinearity, ill-posedness, and high computational costs. Recent advancements leverage machine learning to overcome these issues [2], [3].

Electromagnetic classification [4] involves the categorization or labeling of objects based on their interaction with electromagnetic waves. It is a type of pattern recognition where the goal is to assign predefined classes or categories to objects based on the features extracted from the electromagnetic responses. Unlike inversion, which focuses on recovering the properties of a medium, electromagnetic classification is concerned with identifying or classifying objects themselves, as shown in Fig. 1(c). This can have applications in various fields, including target recognition in radar systems, object identification using electromagnetic sensors, or even classifying materials based on their electromagnetic signatures. Unlike traditional approaches that often involve signal processing [5], this work lies on machine learning-based object classification solely using electromagnetic data. While computer vision has achieved automated recognition, our work explores the potential of classifying objects based on scattered electromagnetic waves, with implications for robotics and environmental perception.

II. Data Set Preparation

The Modified National Institute of Standards and Technology (MNIST) dataset [6], widely employed in machine learning and computer vision, comprises grayscale images of handwritten digits with associated labels. In this work, the 60,000 MNIST images are transformed into a scatterer database, converting pixel intensity values which change between 0 and 255 in the original image files, to relative electrical permittivity values (changing between 1 and 4) via simple linear interpolation. Then, the electromagnetic scattering dataset is generated through a freely available 2D electromagnetic finite difference frequency domain simulation tool called Ceviche [7].

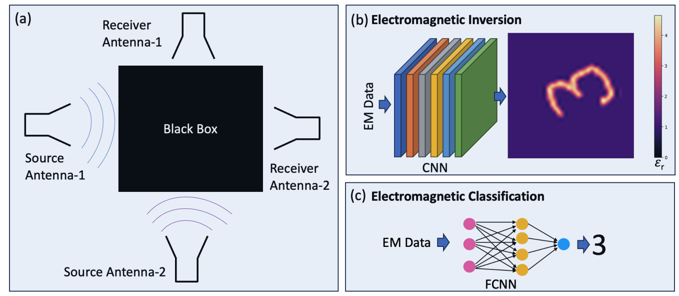

Fig. 1. (a) Schematic illustration of a measurement setup that is typically used in electromagnetic inversion. (b) In electromagnetic inversion, the relative permittivity map is obtained with a CNN. (c) In electromagnetic classification, the output is simply the label (class) of the object.

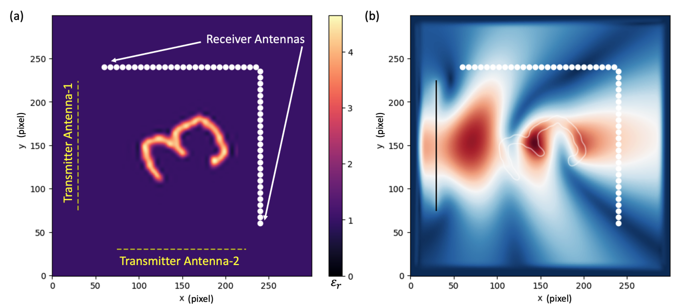

Fig. 2. (a) Permittivity distribution for one of the example geometries studied. The purple regions have a relative permittivity of 1. The regions with higher relative permittivity values are represented by lighter colors. The locations of patch (transmitter) antennas are indicated by yellow dashed lines. (b) The solver calculates electric and magnetic fields all over the computation domain but we only use the data recorded at the 52 locations depicted with white circles.

The computational domain, illustrated in Fig. 2(a) has dimensions of $2\lambda \times 2\lambda$, with uniform meshing along the x and y directions ($\Delta x = \Delta y = \lambda/150$), where λ is the wavelength of electromagnetic waves from a transmitter antenna. Perfectly matched layers with a thickness of $\lambda/7.5$ are incorporated. Initially, the permittivity of each cell is assumed to be 1. The permittivity is then updated in a 140-pixel by 140-pixel region at the domain center using 2D cubic interpolation. Two groups of 26 receiver antennas each are placed at specific locations, and there are two transmitter antennas. The electromagnetic fields (see Fig. 2(b) as an example for the z-component of the electric field intensities) are calculated at 52 receiver antennas for each transmitter antenna, resulting in real and imaginary components stored in a dataset. The dataset's input section has 60,000 rows and 624 columns, representing receiver antennas, transmitter antennas, electromagnetic fields, and components. The output section is a $60,000 \times 1$ vector containing labels (digits). The setup allows for the generation of a comprehensive dataset for training and testing machine learning models in the context of electromagnetic classification.

III. Numerical Results

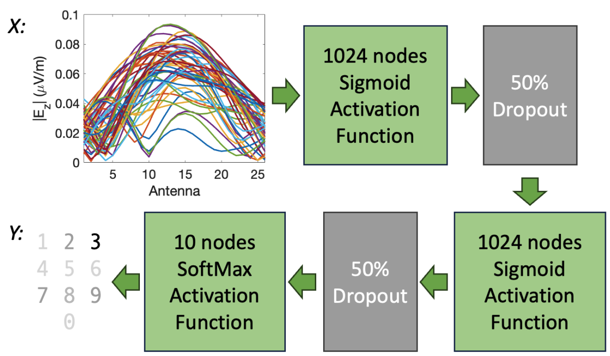

Fig. 3. Neural network architecture.

We utilize the functional application program interface (API) of Keras [8], running on top of TensorFlow [9]. The neural network architecture, illustrated in Fig. 3, is composed of three hidden layers positioned between the input and output layers. The first two layers, each containing 1024 nodes, are succeeded by dropout layers with a 50% dropout rate. This inclusion is to prevent overfitting, enhance model generalization, and bolster the neural network's robustness. The activation function for the initial two layers is the sigmoid function [10], while the last layer encompasses 10 nodes. The SoftMax activation function [11] is applied to this layer, generating probabilities for each label. For classification predictions, the class with the highest probability is selected. The learning rate is set to 10^{-3}, and the optimizer of choice is Adam [12]. Categorical cross-entropy [13] defines the loss function, and the training process is executed over 200 epochs.

For the initial set of calculations, we allocate 50% of the dataset for training and the other 50% for testing, and we obtain an 86 % accuracy in classification. The confusion matrix is provided in Fig. 4. The training takes approximately 21 minutes. To examine the impact of the training dataset size (N_{train}) on accuracy and training time, we conduct an additional set of calculations, varying N_{train} from 600 to 30,000. It is observed that the NN's accuracy increases with the the dataset size as expected. A training data set with 10000 samples guarantees a classification accuracy of 80%, while decreasing the training time by %25.

IV. Conclusion

We have explored the application of neural network techniques in the context of electromagnetic wave-based object

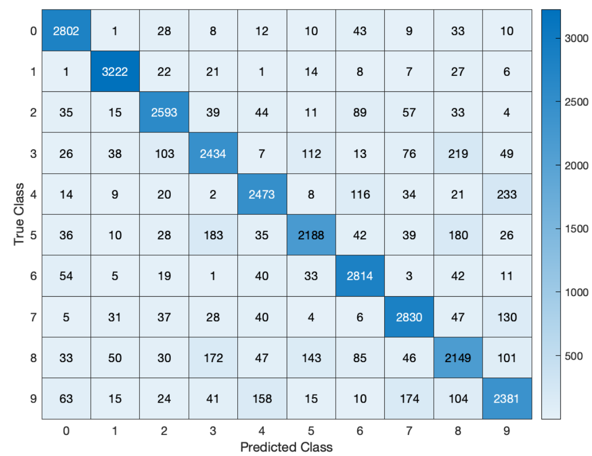

Fig. 4. The confusion matrix.

classification and determined that it is feasible to classify objects with %86 accuracy based on the electromagnetic waves scattered from them in a simple experimental setup.

References

[1] C. Y. Baojun Wei, Ergun Simsek and Q. H. Liu, "Three-dimensional electromagnetic nonlinear inversion in layered media by a hybrid diagonal tensor approximation: Stabilized biconjugate gradient fast fourier transform method," *Waves in Random and Complex Media*, vol. 17, no. 2, pp. 129–147, 2007.

[2] L. Li, L. G. Wang, F. L. Teixeira, C. Liu, A. Nehorai, and T. J. Cui, "Deepnis: Deep neural network for nonlinear electromagnetic inverse scattering," *IEEE Transactions on Antennas and Propagation*, vol. 67, no. 3, pp. 1819–1825, 2019.

[3] K. Xu, L. Wu, X. Ye, and X. Chen, "Deep learning-based inversion methods for solving inverse scattering problems with phaseless data," *IEEE Transactions on Antennas and Propagation*, vol. 68, no. 11, pp. 7457–7470, 2020.

[4] E. Simsek, "Classification with electromagnetic waves," *submitted to IET Microwaves, Antennas & Propagation*, March 2024.

[5] J. A. Zhang, F. Liu, C. Masouros, R. W. Heath, Z. Feng, L. Zheng, and A. Petropulu, "An overview of signal processing techniques for joint communication and radar sensing," *IEEE Journal of Selected Topics in Signal Processing*, vol. 15, no. 6, pp. 1295–1315, 2021.

[6] L. Deng, "The mnist database of handwritten digit images for machine learning research [best of the web]," *IEEE signal processing magazine*, vol. 29, no. 6, pp. 141–142, 2012.

[7] T. W. Hughes, I. A. Williamson, M. Minkov, and S. Fan, "Forward-mode differentiation of maxwell's equations," *ACS Photonics*, vol. 6, no. 11, pp. 3010–3016, 2019.

[8] F. Chollet *et al.*, "Keras," https://keras.io, 2015.

[9] A. Martin *et al.*, "TensorFlow: Large-scale machine learning on heterogeneous systems," 2015, software available from tensorflow.org. [Online]. Available: https://www.tensorflow.org/

[10] D. E. Rumelhart and J. L. McClelland, *Learning Internal Representations by Error Propagation*, 1987, pp. 318–362.

[11] P. Brown, J. Cocke, S. Della Pietra, V. Della Pietra, F. Jelinek, R. Mercer, and P. Roossin, "A statistical approach to language translation," in *Coling Budapest 1988 Volume 1: International Conference on Computational Linguistics*, 1988.

[12] D. P. Kingma and J. Ba, "Adam: A method for stochastic optimization," 2014.

[13] G. Tsoumakas and I. Katakis, "Multi-label classification: An overview," *International Journal of Data Warehousing and Mining (IJDWM)*, vol. 3, no. 3, pp. 1–13, 2007.